Sciencexpress Report

Phasic Firing in Dopaminergic Neurons Is Sufficient for Behavioral Conditioning

Hsing-Chen Tsai,[1,2]* Feng Zhang,[2,]* Antoine Adamantidis,[3] Garret D. Stuber,[4] Antonello Bonci,[4] Luis de Lecea,[3] Karl Deisseroth[2,3]†

1Neuroscience Program, W083 Clark Center, 318 Campus Drive West, Stanford University, Stanford, CA 94305, USA. 2Department of Bioengineering, W083 Clark Center, 318 Campus Drive West, Stanford University, Stanford, CA 94305, USA. 3Department of Psychiatry and Behavioral Sciences, W083 Clark Center, 318 Campus Drive West, Stanford University, Stanford, CA 94305, USA. 4Ernest Gallo Clinic and Research Center, Department of Neurology, Wheeler Center for the Neurobiology of Drug Addiction, University of California San Francisco, San Francisco, CA 94158, USA.

*These authors contributed equally to this work.

†To whom correspondence should be addressed. E-mail: deissero@stanford.edu

Natural rewards and drugs of abuse can alter dopamine signaling, and ventral tegmental area (VTA) dopaminergic neurons are known to fire action potentials tonically (<10Hz) or phasically (15–30Hz) under different behavioral conditions. However, without technology to control specific neurons with appropriate temporal precision in freely-behaving mammals, the causal role of these action potential patterns in driving behavioral changes has been unclear. We used optogenetic tools to selectively stimulate VTA dopaminergic neuron action potential firing in freely behaving mammals. We found that phasic activation of these neurons was sufficient to drive behavioral conditioning and elicited dopamine transients with magnitudes not achieved by longer, lower-frequency spiking. These results demonstrate that phasic dopaminergic activity is sufficient to mediate mammalian behavioral conditioning.

Dopaminergic (DA) neurons have been suggested to be involved in the cognitive and hedonic underpinnings of motivated behaviors (*1-4*). Changes in the firing pattern of DA neurons between low frequency tonic activity (<10 Hz) and phasic bursts of action potentials (15-30 Hz) could encode reward prediction errors and incentive salience (*5*). Consistent with the reward prediction-error hypothesis, DA neuron firing activity is depressed by aversive stimuli (*6*). However, it remains unclear whether DA neuron activation alone is sufficient to elicit reward-related behaviors. Lesion, electrical stimulation, and psychopharmacology studies have been important but have not allowed causal and temporally precise control of DA neurons in freely moving mammals; for example, electrical stimulation will inevitably activate multiple classes of neurons within heterogeneous brain tissue, and pharmacological stimulation will not allow delivery of defined patterns of DA neuron spikes *in vivo*. To control DA neurons selectively, we employed a Cre-inducible adeno-associated virus (AAV) vector (*7, 8*) carrying the gene encoding the light-activated cation channel channelrhodopsin-2 (ChR2) in-frame fused to enhanced yellow fluorescent protein (ChR2-EYFP) (*9, 10*). To ensure that there would be no significant expression leak in non-targeted cell types, we designed the Cre-inducible AAV vector with a double-floxed inverted open reading frame (ORF), wherein the ChR2-EYFP sequence is present in the antisense orientation (Fig. 1A). Stereotactic delivery of this vector into the VTA of tyrosine hydroxylase (TH)::IRES-Cre transgenic mice enables DA neuron-specific expression of ChR2-EYFP. Upon transduction, Cre-expressing TH cells invert the ChR2-EYFP ORF in irreversible fashion and thereby activate sustained ChR2-EYFP expression under the strong, constitutively-active EF-1α promoter.

We validated the specificity and efficacy of this targeting strategy *in vivo*. In coronal VTA sections of transduced TH::IRES-Cre brains, ChR2-EYFP specifically co-localized with endogenous TH (Fig. 1B). Greater than 90% of TH-immunopositive cells were positive for ChR2-EYFP near virus injection sites and more than 50% were positive overall, demonstrating highly efficacious transduction of the TH cells. 98.3±0.5% of ChR2-EYFP expressing cells were co-labeled by TH staining (Fig. 1C), demonstrating high specificity. Expression was stable and persistent for at least 2 months, and ChR2-EYFP expressing neurons displayed robust projections; EYFP-positive fibers richly innervated local neurons in downstream nucleus accumbens (NAcc) (Fig. 1D) (*11*).

To assess the potential for optogenetic control of transduced cells, we used whole-cell patch clamp to measure light-induced membrane currents in ChR2-expressing DA neurons (Fig. 2A). ChR2-EYFP expressing cells in the VTA displayed typical electrophysiological properties of DA neurons with mean resting membrane potential of -56.0±1.8 mV and membrane resistance of 372.3±19.3 MΩ (n = 10

cells), consistent with previously reported values for VTA DA neurons (*12*) and indicating that expression of ChR2 alone does not affect their basic physiology. Under blue light (473 nm) illumination, all patched cells exhibited prominent inward photocurrents (Fig. 2B, C; $n = 10$ cells). Trains of light flashes drove action potential firing in ChR2-EYFP neurons; using low and high frequency light trains, we evoked tonic and phasic DA neuron firing respectively (Fig. 2D). DA neurons typically do not maintain high-frequency spiking (*13*); 1-5 Hz light pulses drove long DA neuron spike trains reliably, while bursting at 20 Hz or greater for prolonged trains evoked action potentials in <50% of light pulses (Figs. 2E, S1; bursts maintaining the >15 Hz spiking characteristic of phasic firing could be elicited simply by using higher frequency light pulse trains). Optrode recording confirmed that optical stimulation of VTA DA neurons *in vivo* evoked broad spike waveforms consistent with extracellular waveforms for VTA DA neurons (*6*) (Fig. 2F; fig. S2).

We next tested the behavioral conditioning effects of phasic DA neuron activity via conditioned place preference (CPP) (Fig. 3A, fig. S3), using phasic optogenetic stimulation (*14*) of DA neurons as our conditioning stimuli (Fig. 3B, C). As a control, we paired the opposite chamber with the same number of light pulses delivered instead at 1 Hz. Mice were subjected to 2 days of conditioning, and conditioned preference was determined by comparing time spent in each chamber of the apparatus. In the first round of experiments, mice received phasic (50Hz optical stimulation) conditioning in one chamber on the first day of conditioning (day 2), and 1Hz optical stimulation in the other chamber on the second day of conditioning (day 3); two cohorts of mice were used with the chamber/stimulation pairing reversed to control for spontaneous preference shifts (fig. S3). Mice developed a clear place preference for the chamber associated with phasic optical stimulation by several measures (Fig. 3D-F; $p<0.001$ by Student's *t*-test; $n=13$ mice), and both cohorts of mice exhibited this conditioned preference independent of chamber pairing (fig. S5).

We performed two classes of control experiments to validate the results. First, non-transgenic littermates ($n = 9$) were injected with the Cre-dependent ChR2-EYFP AAV and subjected to the same stimulation paradigm as the experimental animals. Separately, TH::IRES-Cre transgenic mice ($n = 9$) were injected with the Cre-dependent ChR2-EYFP AAV but received no optical stimulation during conditioning to further control for spontaneous preference shifts. Neither control group showed a significant conditioned chamber preference (Fig. 3E right, $p>0.5$ by Student's *t*-test). Furthermore, we did not find any significant changes in anxiety-related behaviors (Fig. 3G) or in locomotor activity (Fig. 3H) during preference tests and in open field tests (fig. S6).

Next, we tested whether the place preference effect observed was due to an appetitive effect from 50Hz stimulation, or to an aversive effect from 1Hz stimulation. We compared the effect of each firing modality with no stimulation, in two independent cohorts. Consistent with the previous CPP experiments (Fig. 3E,F), the phasic cohort displayed significant place preference for the stimulation chamber after conditioning (Fig. 4A,C), from 251±28s during pre-test to 522±63s during post-test ($n=7$ mice; $p<0.05$, Student's *t*-test). However the 1Hz cohort showed no place aversion for the 1Hz stimulation chamber (showing a trend toward place preference for 1Hz instead; Fig. 4B, C). We hypothesized that the CPP effect observed for the phasic cohort could be due to larger transient DA release triggered by the 50Hz optical stimulation. We therefore used *in vivo* fast-scan cyclic voltammetry (FSCV) (*15, 16*) to detect DA transients. Maintaining the optical fiber in the VTA, we implanted a carbon fiber electrode for measuring DA signals in the NAcc, one of the major targets of VTA DA projections (Fig. 1D). Despite sharing the same total illumination duration and number of light flashes (25 15ms light flashes at 1Hz or 50Hz), the 50Hz light train elicited larger DA transients (Fig. 4D,E). Indeed, the mean peak DA transient concentrations in the NAcc were measured at 75.9±24.5 nM and 1.3±0.8 nM respectively for the 50Hz and 1Hz stimuli (Fig. 4E); the former is similar to the magnitude of natural reward-triggered dopamine transients (*15*), while DA accumulation during chronic 1Hz stimulation remained much lower (fig. S7; this level of DA could still theoretically contribute to behavioral changes).

Rodents learn to associate the effects of stimuli with their environment, and subsequently display a conditioned place preference for that environment (*17*). Previous studies have demonstrated the important role of DA in the processing of salient signals (*18*) and goal-directed behaviors (*19*). However it has been unclear if other circuits and neurotransmitter systems are required at the same time (*20*), and which patterns of activity in which neuron types are sufficient to drive place preference. To enable direct testing of the role of phasic DA neuron firing on conditioned behaviors, we developed a versatile Cre-inducible gene-expression system to decouple the strength of transgene expression from cell type-specific promoters (which are often too weak to drive functional expression of opsins). Using this system, we selectively modulated DA neuron activity with defined stimulation patterns in the CPP paradigm, and found that phasic stimulation sufficed to establish place preference in the absence of other reward. These results establish a causal role in behavioral conditioning for defined spiking modes in a specific cell type; of course, even a single cell

type can release multiple neurotransmitters and neuromodulators (for example, VTA DA neurons primarily release DA but can also release other neurotransmitters such as glutamate) and will exert effects through multiple distinct downstream cell types. Indeed, the optogenetic approach, integrated with electrophysiological, behavioral, and electrochemical readout methods, opens the door to exploring the causal, temporally-precise, and behaviorally relevant interactions of DA neurons with other neuromodulatory circuits (*21–24*), including monoaminergic and opioid circuits important in neuropsychiatric illnesses (*25–27*). In the process of identifying candidate interacting neurotransmitter systems, downstream neural circuit effectors (*28*), and subcellular biochemical mechanisms on timescales appropriate to behavior and relevant circuit dynamics, it will be important to continue to leverage the specificity and temporal precision of optogenetic control (*29*).

References and Notes

1 R. A. Wise, *Nat Rev Neurosci* **5**, 483 (2004).
2. B. J. Everitt, T. W. Robbins, *Nat Neurosci* **8**, 1481 (2005).
3. T. E. Robinson, K. C. Berridge, *Brain Res Brain Res Rev* **18**, 247 (1993).
4. G. F. Koob, M. Le Moal, *Science* **278**, 52 (1997).
5. W. Schultz, *Annu Rev Neurosci* **30**, 259 (2007).
6. M. A. Ungless, P. J. Magill, J. P. Bolam, *Science* **303**, 2040 (2004).
7. F. Zhang, in *Larry M. Katz Memorial Lecture, Cold Spring Harbor Laboratory Meeting on Neuronal Circuits*. (Cold Spring Harbor Laboratory, March 2008).
8. D. Atasoy, Y. Aponte, H. H. Su, S. M. Sternson, *J Neurosci* **28**, 7025 (2008).
9. E. S. Boyden, F. Zhang, E. Bamberg, G. Nagel, K. Deisseroth, *Nat Neurosci* **8**, 1263 (2005).
10. G. Nagel *et al.*, *Proc Natl Acad Sci U S A* **100**, 13940 (2003).
11. A. Bjorklund, S. B. Dunnett, *Trends Neurosci* **30**, 194 (2007).
12. Q. S. Liu, L. Pu, M. M. Poo, *Nature* **437**, 1027 (2005).
13. S. Robinson, D. M. Smith, S. J. Mizumori, R. D. Palmiter, *Proc Natl Acad Sci U S A* **101**, 13329 (2004).
14. A. R. Adamantidis, F. Zhang, A. M. Aravanis, K. Deisseroth, L. de Lecea, *Nature* **450**, 420 (2007).
15. P. E. Phillips, G. D. Stuber, M. L. Heien, R. M. Wightman, R. M. Carelli, *Nature* **422**, 614 (2003).
16. G. D. Stuber *et al.*, *Science* **321**, 1690 (2008).
17. T. M. Tzschentke, *Addict Biol* **12**, 227 (2007).
18. C. M. Cannon, R. D. Palmiter, *J Neurosci* **23**, 10827 (2003).
19. A. A. Grace, S. B. Floresco, Y. Goto, D. J. Lodge, *Trends Neurosci* **30**, 220 (2007).
20. T. S. Hnasko, B. N. Sotak, R. D. Palmiter, *J Neurosci* **27**, 12484 (2007).
21. P. W. Kalivas, *Am J Addict* **16**, 71 (2007).
22. M. R. Picciotto, W. A. Corrigall, *J Neurosci* **22**, 3338 (2002).
23. J. A. Dani, D. Bertrand, *Annu Rev Pharmacol Toxicol* **47**, 699 (2007).
24. G. C. Harris, G. Aston-Jones, *Neuropsychopharmacology* **28**, 865 (2003).
25. E. J. Nestler, W. A. Carlezon, Jr., *Biol Psychiatry* **59**, 1151 (2006).
26. J. Williams, P. Dayan, *J Child Adolesc Psychopharmacol* **15**, 160 (2005).
27. A. M. Graybiel, *Annu Rev Neurosci* **31**, 359 (2008).
28. W. Shen, M. Flajolet, P. Greengard, D. J. Surmeier, *Science* **321**, 848 (2008).
29. F. Zhang *et al.*, *Nature* **446**, 633 (2007).

30. We thank Mark Wightman, Paul Phillips, and the entire Deisseroth lab for their support. H.C.T is supported by a Stanford Graduate Fellowship. F.Z. and G.D.S. are supported by NIH NRSA grants. A.R.A. is supported by the Fonds National de la Recherche Scientifique, NARSAD and the Fondation Leon Fredericq. L.d.L. is supported by NIDA, DARPA and NARSAD. K.D. is supported by McKnight, Coulter, NSF, NIMH, NIDA, and the Snyder, Albert Yu and Mary Bechmann, and Keck Foundations.

Supporting Online Material

www.sciencemag.org/cgi/content/full/1168878/DC1
Materials and Methods
Figs. S1 to S7
References

24 November 2008; accepted 7 April 2009
Published online 23 April 2009; 10.1126/science.1168878
Include this information when citing this paper.

Fig. 1 Specific ChR2 expression in DA neurons. (**A**) Schematic of the Cre-dependent AAV; the gene of interest is doubly flanked by two sets of incompatible lox sites. Upon delivery into TH::IRES-Cre transgenics, ChR2-EYFP is inverted to enable transcription from the EF-1α promoter. (**B**) Confocal images showing cell-specific ChR2-EYFP expression (green) in TH neurons (red). (**C**) Statistics of expression in TH neurons ($n = 491$); error bars represent s.e.m. throughout. (**D**) Labeled VTA DA neurons project to downstream brain regions; confocal images of ChR2-EYFP positive axons (green) innervating target neurons in NAcc (NeuN, red).

Fig. 2 Photoactivation of DA neurons in intact tissue. (**A**) Recording from transduced neurons in acute VTA slices.

Recorded neurons are verified by intracellular dye loading (ChR2-EYFP, green; AlexaFluor 594, red). (**B**) Continuous blue light (473nm) evoked inward photocurrents. (**C**) Summary of photocurrent properties (n = 10). (**D**) Whole-cell recording of DA neurons showing spontaneous activity and tonic and phasic firing evoked by 1Hz and 50Hz light flash trains, respectively (25 flashes, 15 ms per flash) (**E**) Light-evoked spike trains are reliable over a range of frequencies; percentage of action potentials evoked by 25 light flashes at indicated frequencies (1-50 Hz) is shown (n = 7). (**F**) In vivo optrode recording of VTA DA neurons in a transduced TH::IRES-Cre anaesthetized mouse showing light-evoked DA spikes; see fig. S2. (Inset) Typical triphasic DA extracellular spike.

Fig. 3 Photoactivation of DA neurons induces place preference. (**A**) CPP timeline (see also fig. S3). (**B**) Light delivery parameters; 25-flashes at 1 or 50 Hz were delivered with a periodicity of 1 min. (**C**) Optical fiber is inserted through a cannula guide implanted over the VTA to photoactivate DA neurons. (**D**) Representative density maps showing conditioned preference; pseudo-color represents duration at each position. (**E**) Conditioning effect of DA neuron modulation. (Left) Comparison of time in each chamber during pre-test (white) and post-test (gray). (Right) Comparison of preference scores for experimental (time in phasic chamber as a fraction of total time in side chambers) and control cohorts (Phasic Stim, n = 13; No Stim, n = 9; Littermate, n = 9). (**F**) Difference scores (calculated as the difference between time spent during pre- and post-test in the specified chamber) for each chamber shows a statistically significant shift in preference. (**G**) Analysis of anxiety (fractional time in center of a chamber; n = 13). (**H**) Chamber entries, long-range locomotion (different sequential beam-breaks), and short-range locomotion (repeated break of the same beam) during pre- and post-test (n = 13). *P<0.05, **P<0.01, ***P<0.001.

Fig. 4 Phasic DA neuron stimulation leads to transient DA release and place preference. (**A**, **B**) Effect of phasic (50Hz) (A) and tonic (1Hz) (B) stimulation on place preference. (Left), time spent in each chamber during preference test. (Right), comparison of preference scores; A: n = 7, B: n = 6). (**C**) Relative effects of stimulation frequency examined using the difference scores for phasic, tonic, and non-associative control (same as No Stim in Fig. 3E) cohorts. (**D**) FSCV measurements of VTA stimulation-triggered transient DA release in NAcc in anesthetized TH::IRES-Cre mice. (Top) Representative voltammetry traces during phasic (25 flashes/50 Hz) and tonic (16 flashes/1 Hz) stimulation of VTA. (Insets) Background-subtracted voltammogram taken from the peak of stimulation, indicating that signal measured is DA based on comparison to voltammograms of DA obtained in vitro. (Bottom) All background-subtracted voltammograms recorded over the 20s interval. Y-axis: applied potential (E_{apps} vs. Ag/AgCl reference electrode; X-axis: the time at which each voltammogram was recorded. Current changes at the electrode are encoded in color. DA can be seen during stimulation at the feature ~0.650V (oxidation peak encoded as green) and between ~−0.20 V and ~−0.25 V at the end of the voltage scan. (**E**) Comparison of phasic and tonic light-evoked DA transients (n = 3). *P<0.05.

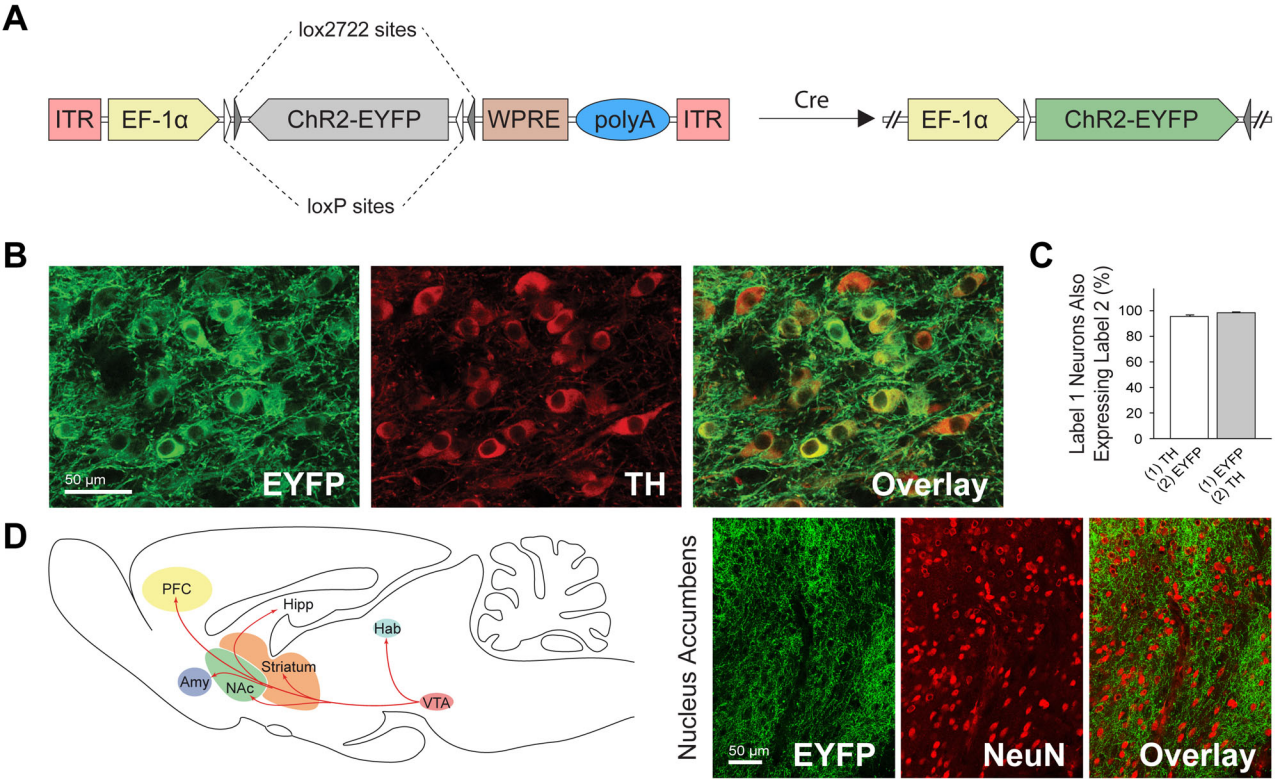
A
lox2722 sites
ITR
EF-1α
ChR2-EYFP
WPRE
polyA
ITR
loxP sites
Cre
EF-1α
ChR2-EYFP
B
50 µm
EYFP
TH
Overlay
C
Label 1 Neurons Also Expressing Label 2 (%)
100
80
60
40
20
0
(1) TH (2) EYFP
(1) EYFP (2) TH
D
PFC
Hipp
Hab
Striatum
Amy
NAc
VTA
Nucleus Accumbens
50 µm
EYFP
NeuN
Overlay

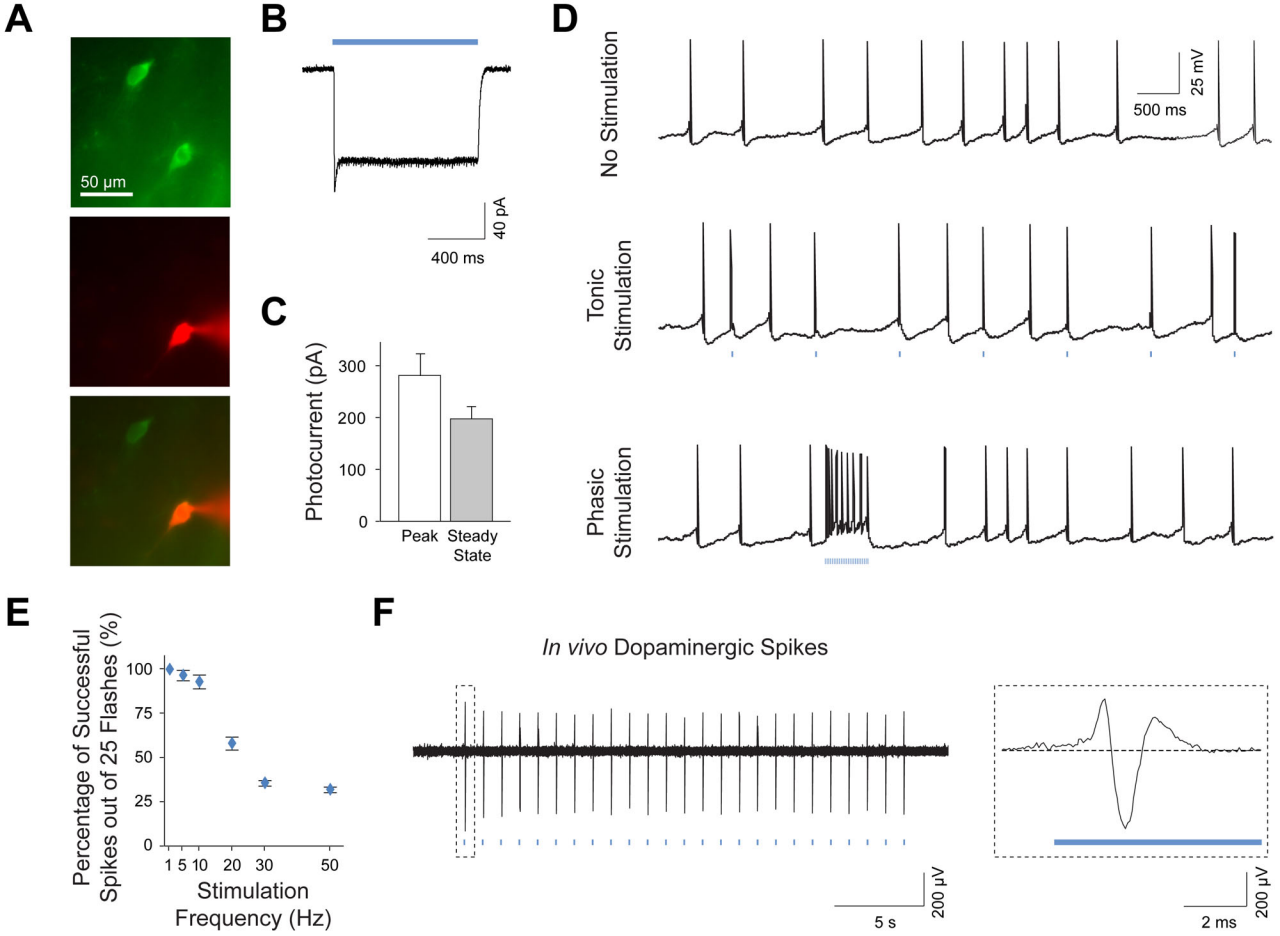
A
50 µm
B
40 pA
400 ms
C
Photocurrent (pA)
300
200
100
0
Peak
Steady State
D
No Stimulation
25 mV
500 ms
Tonic Stimulation
Phasic Stimulation
E
Percentage of Successful Spikes out of 25 Flashes (%)
100
75
50
25
0
1 5 10 20 30 50
Stimulation Frequency (Hz)
F
In vivo Dopaminergic Spikes
200 µV
5 s
2 ms
200 µV

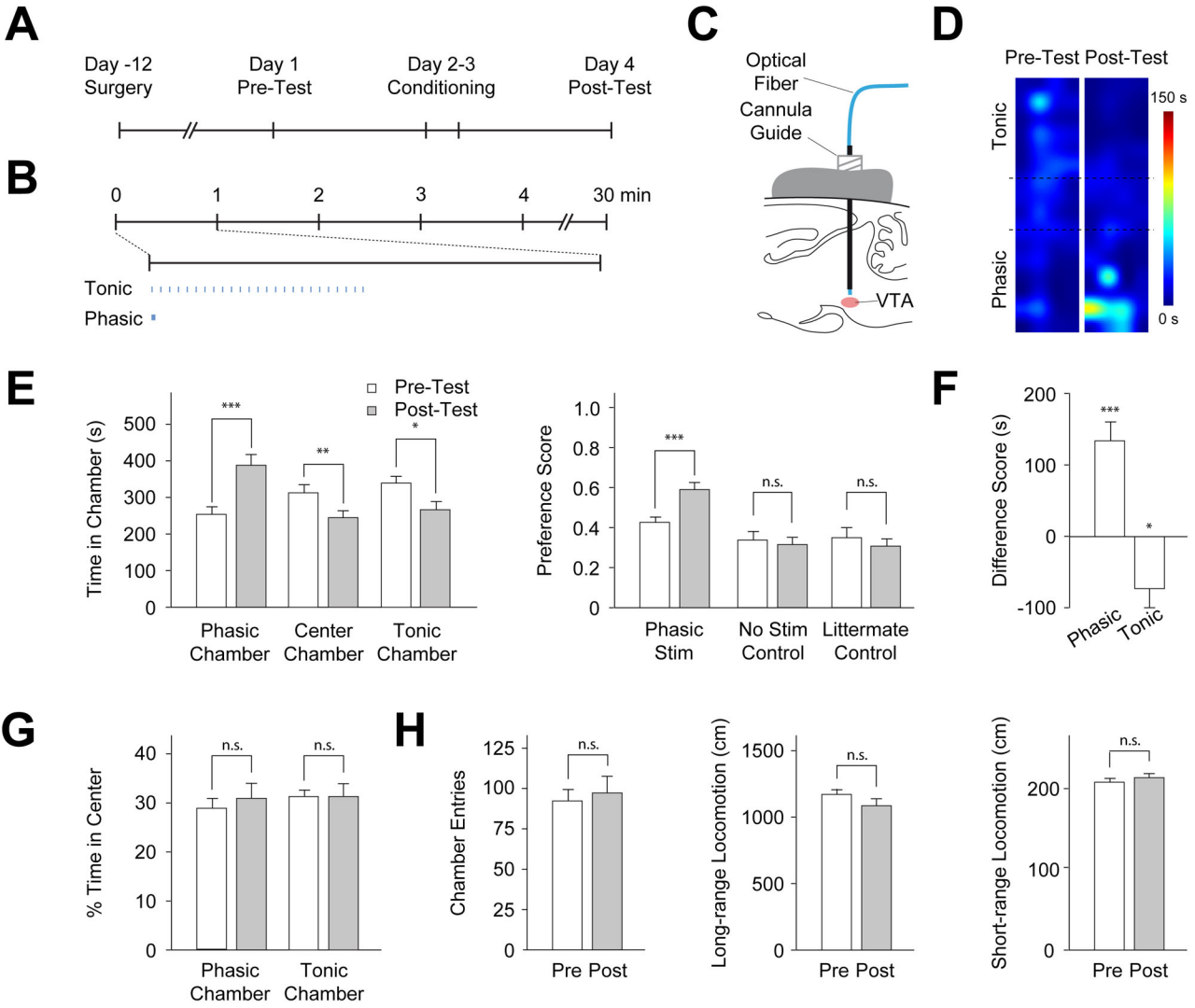
A
Day -12
Surgery
Day 1
Pre-Test
Day 2-3
Conditioning
Day 4
Post-Test
B
0
1
2
3
4
30 min
Tonic
Phasic
C
Optical
Fiber
Cannula
Guide
VTA
D
Pre-Test Post-Test
Tonic
Phasic
150 s
0 s
E
Pre-Test
Post-Test
Time in Chamber (s)
Phasic
Chamber
Center
Chamber
Tonic
Chamber
Preference Score
Phasic
Stim
No Stim
Control
Littermate
Control
n.s.
F
Difference Score (s)
Phasic
Tonic
G
% Time in Center
Phasic
Chamber
Tonic
Chamber
H
Chamber Entries
Pre Post
Long-range Locomotion (cm)
Short-range Locomotion (cm)

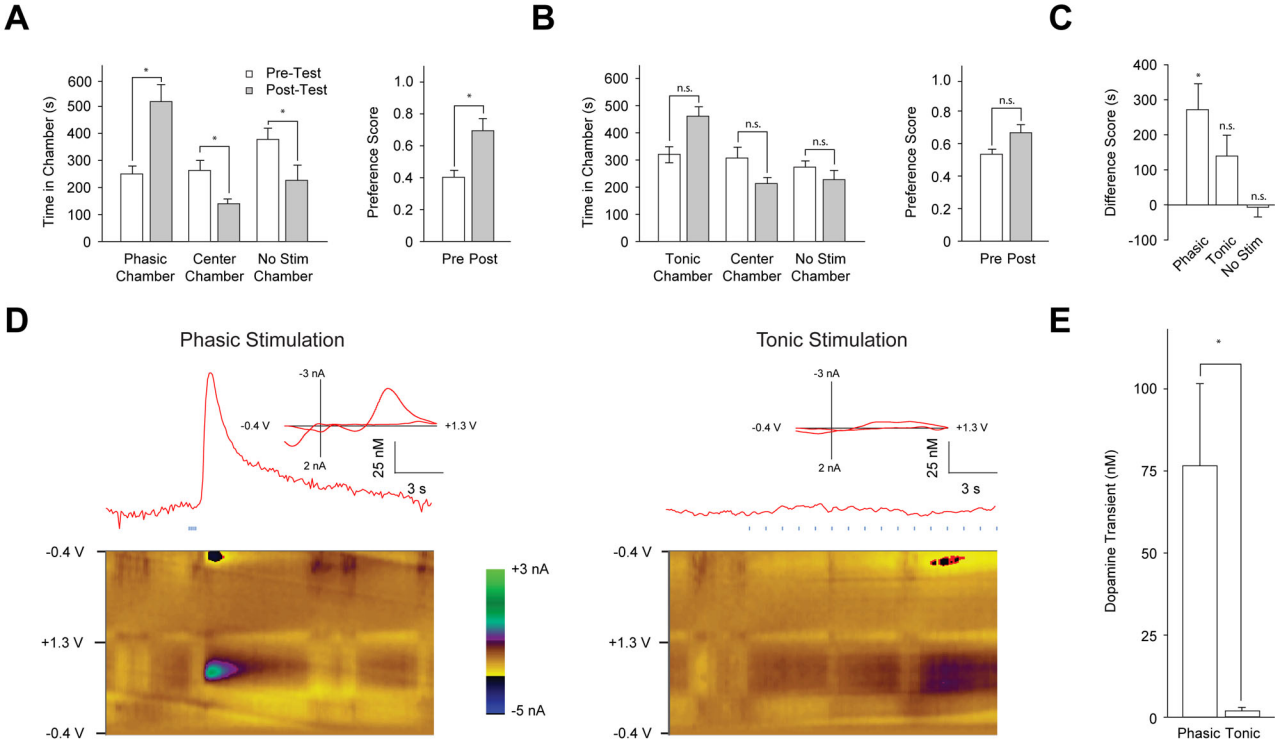
A
Time in Chamber (s)
Pre-Test
Post-Test
Phasic Chamber
Center Chamber
No Stim Chamber
Preference Score
Pre Post
B
Time in Chamber (s)
n.s.
Tonic Chamber
Center Chamber
No Stim Chamber
Preference Score
Pre Post
C
Difference Score (s)
Phasic
Tonic
No Stim
D
Phasic Stimulation
-3 nA
-0.4 V
+1.3 V
2 nA
25 nM
3 s
+3 nA
-5 nA
Tonic Stimulation
E
Dopamine Transient (nM)
Phasic
Tonic